The 1st Joint International Conference on Multibody System Dynamics
May 25–27, 2010, Lappeenranta, Finland

Structure preserving optimal control simulation of index finger dynamics

Ramona Maas*, Sigrid Leyendecker *

* Computational Dynamics and Control
University of Kaiserslautern
PO Box 3049
D-67653 Kaiserslautern, Germany
e-mail: rmaas@rhrk.uni-kl.de, leyendecker@rhrk.uni-kl.de

ABSTRACT

Trajectory planning of human motion is done unconsciously by the central nervous system (CNS). To get a better understanding about how the human CNS controls movements in a particular example, we investigate the trajectory of the index finger during grasping. In this regard, we describe the index finger, which consists of three phalanxes and three connecting joints, as an n-dimensional forced constrained multibody system. Varying forefinger movements are formulated as optimal control problems for constrained motion. At this stage, the actuation of the finger due to muscles is simply represented by bounded joint torques. However, the inclusion of muscle models is planned for the future. For the solution of the optimal control problem, DMOCC (Discrete Mechanics and Optimal Control for Constrained Systems, introduced in [8]) is used. DMOCC can be classified as a direct method, thus transforming the optimal control problem into a constrained optimisation problem. The algorithm yields a sequence of discrete configurations together with a sequence of actuating controls being optimal in the sense of minimising an objective function while the described (in-)equality constraints, and most importantly, the discrete equations of motion are fulfilled. Their structure preserving formulation distinguishes DMOCC from other direct transcription methods. It guarantees that certain characteristic properties of the real motion are inherited by the approximate trajectory. For example, the evolution of the systems momentum maps exactly represents externally applied controls and energy is not dissipated artificially. This is crucial, since numerical dissipation would lead to over- or underestimation of the joint torques. As in [4], the motion due to different objective functions like total control effort, torque change, kinetic energy and jerk in the fingertip is compared.

Keywords: grasping, DMOCC, index finger movement, physiologically motivated cost function.

1 INTRODUCTION

Human movements, in particular grasping movements, are known to be mostly controlled unconsciously by our central nervous system (CNS), see e.g. [13]. The question of how our CNS controls our movements and which criteria are used to choose a trajectory for instance during grasping, has been a research topic for a long time. In this work, we simulate grasping movements of the index finger.
The index finger consists of three phalanxes, phalanx proximalis, media and distalis, that are connected by different joints, as illustrated in Figure 1, see [5]. These bones and joints have been analysed in several publications with respect to their shape and dimension. For example in [3], a method has been developed to derive several finger dimensions as a function of external hand measurements. The metacarpo-phalangeal joint (MCP) connecting the metacarpal bone with the first phalanx is a spherical joint with three rotational degrees of freedom of which only two, adduction-abduction and flexion-extension, can be actively controlled by muscles and tendons. The third rotational degree of freedom in this joint, rotation about its longitudinal axis, can only be passively activated as for example in case of crooked pressing of buttons. The proximal inter-phalangeal joint and the distal inter-phalangeal joint, combining the medial and distal phalanxes to the finger, allow rotation around one axis to perform flexion-extension only.
Thus simplifying, the human index finger, consisting of several bones connected by joints, can be modelled as an n-dimensional constrained forced multibody system. The system is subject to constraints because of the employed rigid body formulation and the joints in between the bodies. Furthermore, it is forced by actuation in the joints. Therefore, the dynamical behaviour of the system can be described via its Lagrangian,

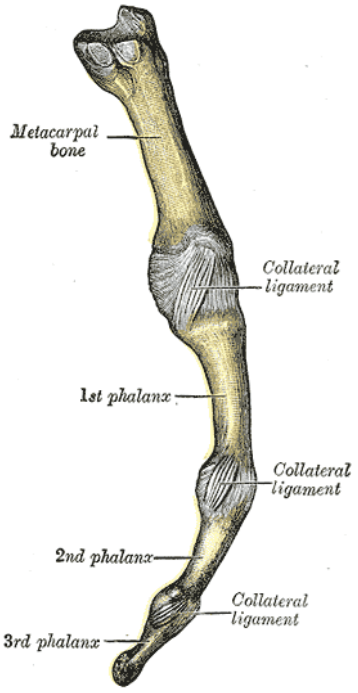

Figure 1. Texture of the index finger with bones and joints overlaid by ligaments [5].

constraints and forces. However, the configuration and control trajectories are unknown, thus there is an infinite number of possible trajectories, the index finger could use to reach a specified target point. Hence, a possibility to find trajectories is to formulate the index finger movement as an optimal control problem of an n-dimensional constrained forced multibody system, using a physiologically motivated cost function.

There has been a lot of research on that topic and several models for the description of how our CNS controls movements have been developed. Especially in arm movements, energetic considerations like minimising cost functions related to kinetic energy or change in torques have led to promising models [12, 2]. In [4], finger movements during grasping have been in the focus and they found a minimum angular jerk in fingertip criterion as best fitting their experimental results. However, all the mentioned works neglect the influence of gravity on the movements. For example in [2] it is assumed, that all acting muscle torques can be additively split into a driving torque and a torque that counteracts gravity. Then, they neglect the influence of gravity an the counteracting part of the torques.

In this work, we investigate index finger movements and their control by the CNS similar to [4], but from a slightly more general point of view by additionally taking the influence of gravity into account. Furthermore, what distinguishes this work form existing work on the simulation of human motion is the use of structure preserving numerical methods. Most importantly, we use discrete equations of motion, that preserve the characteristics of the real system, for example symplecticity or momentum maps (in particular angular momentum in the index finger example) are represented consistently in the numerical simulation and energy is not artificially dissipated. Many common numerical integrators, like for example the implicit or explicit Euler algorithm, artificially loose or gain energy during numerical simulations. For our application, it is crucial, that the structure of the system is preserved, as an optimisation related to energy or torques can only lead to reasonable results, if these quantities are represented in an accurate manner. Thus, we use a structure preserving formulation of our optimal control problem called DMOCC, as introduced in [8]. In the formulation of the optimal control problem, we use four different physiologically motivated cost functions and compare them to the results of [6], where it is stated that fingers tend to follow a particularly curved trajectory during grasping movements that can be described by a logarithmic spiral.

2 FORWARD DYNAMICS

2.1 Constrained forced dynamics

To simulate grasping movements of the index finger, we perform a dynamic simulation of an n-dimensional forced, constrained multibody system with its configuration defined by $\boldsymbol{q}(t) \in Q \subseteq \mathbb{R}^n$ in a configuration manifold Q with velocity $\dot{\boldsymbol{q}}(t) \in T_{\boldsymbol{q}(t)}Q$. Here, t denotes the time variable in the bounded interval $[t_0, t_N] \subset \mathbb{R}$. As described in [8], the constrained version of the principle of Lagrange d'Alembert yields

$$\delta \int_{t_0}^{t_N} L(\boldsymbol{q}, \dot{\boldsymbol{q}}) - \boldsymbol{g}^T(\boldsymbol{q}) \cdot \boldsymbol{\lambda}\, dt + \int_{t_0}^{t_N} \boldsymbol{f} \cdot \delta \boldsymbol{q}\, dt = 0 \tag{1}$$

for all variations $\delta \boldsymbol{q} \in TQ$ vanishing at endpoints and $\delta \boldsymbol{\lambda} \in \mathbb{R}^m$. Here, $L(\boldsymbol{q}, \dot{\boldsymbol{q}})$ is the Lagrangian of the system, which is defined as the difference between kinetic and potential energy and the motion is constrained

by the vector valued function of holonomic, scleronomic constraints $\boldsymbol{g}(\boldsymbol{q}) = \boldsymbol{0} \in \mathbb{R}^m$, resulting from the rigid body formulation and the joints in between the bodies, see [1, 7]. Additionally, $\boldsymbol{\lambda}(t)$ represents the vector of time-dependent Lagrange multipliers. The last term in (1) contains the non-conservative forces $\boldsymbol{f} \in \mathbb{R}^n$ that actuate the system and represents their virtual work. Straight forward calculations lead to the $(n+m)$-dimensional differential-algebraic system of equations of motion for constrained forced systems

$$\begin{aligned} \frac{\partial L(\boldsymbol{q}, \dot{\boldsymbol{q}})}{\partial \boldsymbol{q}} - \frac{d}{dt}\left(\frac{\partial L(\boldsymbol{q}, \dot{\boldsymbol{q}})}{\partial \dot{\boldsymbol{q}}}\right) - \boldsymbol{G}^T(\boldsymbol{q}) \cdot \boldsymbol{\lambda} + \boldsymbol{f} &= \boldsymbol{0} \\ \boldsymbol{g}(\boldsymbol{q}) &= \boldsymbol{0} \end{aligned} \tag{2}$$

with $\boldsymbol{G}(\boldsymbol{q}) = D\boldsymbol{g}(\boldsymbol{q})$ denoting the Jacobian of the constraints.

2.2 Discrete constrained forced dynamics

Instead of discretising the equations of motion (2), following the discrete mechanics approach, a discrete version is derived via a discrete variational principle. This naturally leads to a structure preserving version of discrete equations of motion, which inherits characteristics like symplecticity and the conservation of momentum maps from the analytical system, as shown in the discrete Noether's Theorem in [10]. According to [7, 8] we approximate the first term of equation (1) in a time interval $[t_n, t_{n+1}]$ using the discrete Lagrangian $L_d : Q \times Q \to \mathbb{R}$ as follows

$$L_d(\boldsymbol{q}_n, \boldsymbol{q}_{n+1}) - \frac{\Delta t}{2}\left(\boldsymbol{g}^T(\boldsymbol{q}_n) \cdot \boldsymbol{\lambda}_n + \boldsymbol{g}^T(\boldsymbol{q}_{n+1}) \cdot \boldsymbol{\lambda}_{n+1}\right) \approx \int_{t_n}^{t_{n+1}} L(\boldsymbol{q}, \dot{\boldsymbol{q}}) - \boldsymbol{g}^T(\boldsymbol{q}) \cdot \boldsymbol{\lambda}\, dt$$

In this work, the discrete Lagrangian $L_d(\boldsymbol{q}_n, \boldsymbol{q}_{n+1})$ is approximated by the midpoint rule and a constant time step $\Delta t = t_{n+1} - t_n$ is used. The virtual work is similarly approximated via

$$\boldsymbol{f}_n^- \cdot \delta\boldsymbol{q}_n + \boldsymbol{f}_n^+ \cdot \delta\boldsymbol{q}_{n+1} \approx \int_{t_n}^{t_{n+1}} \boldsymbol{f} \cdot \delta\boldsymbol{q}\, dt$$

With these approximations, the discrete version of the constrained Lagrange-d'Alembert principle (1) states that

$$\delta \sum_{n=0}^{N-1} L_d(\boldsymbol{q}_n, \boldsymbol{q}_{n+1}) - \frac{\Delta t}{2}\left(\boldsymbol{g}^T(\boldsymbol{q}_n) \cdot \boldsymbol{\lambda}_n + \boldsymbol{g}^T(\boldsymbol{q}_{n+1}) \cdot \boldsymbol{\lambda}_{n+1}\right) + \sum_{n=0}^{N-1} \boldsymbol{f}_n^- \cdot \delta\boldsymbol{q}_n + \boldsymbol{f}_n^+ \cdot \delta\boldsymbol{q}_{n+1} = 0$$

for all variations $\{\delta\boldsymbol{q}_n\}_{n=0}^N$ and $\{\delta\boldsymbol{\lambda}_n\}_{n=0}^N$ with $\delta\boldsymbol{q}_0 = \delta\boldsymbol{q}_N = \boldsymbol{0}$, which directly leads to the discrete constrained forced Euler-Lagrange equations of motion

$$\begin{aligned} D_2 L_d(\boldsymbol{q}_{n-1}, \boldsymbol{q}_n) + D_1 L_d(\boldsymbol{q}_n, \boldsymbol{q}_{n+1}) - \Delta t\, \boldsymbol{G}^T(\boldsymbol{q}_n) \cdot \boldsymbol{\lambda}_n + \boldsymbol{f}_{n-1}^+ + \boldsymbol{f}_n^- &= \boldsymbol{0} \\ \boldsymbol{g}(\boldsymbol{q}_{n+1}) &= \boldsymbol{0} \end{aligned} \tag{3}$$

The dimension of this discrete system of equations is $(n+m)$ as in the continuous case. It is important to note, that (3) has not been obtained via discretisation of (2) but rather via a discrete variational principle.

Discrete null space method

Reduction of the system to a lower dimension is possible by premultiplication of (3) with a discrete null space matrix fulfilling

$$\text{range}\,(\boldsymbol{P}(\boldsymbol{q}_n)) = \text{null}\,(\boldsymbol{G}(\boldsymbol{q}_n))$$

see [1, 7]. In doing so, the constrained forces and therefore the unknown Lagrange multipliers vanish from the discrete equations of motion (3) and the systems dimension is reduced to n. This yields

$$\begin{aligned} \boldsymbol{P}^T(\boldsymbol{q}_n) \cdot \left(D_2 L_d(\boldsymbol{q}_{n-1}, \boldsymbol{q}_n) + D_1 L_d(\boldsymbol{q}_n, \boldsymbol{q}_{n+1}) + \boldsymbol{f}_{n-1}^+ + \boldsymbol{f}_n^-\right) &= \boldsymbol{0} \\ \boldsymbol{g}(\boldsymbol{q}_{n+1}) &= \boldsymbol{0} \end{aligned} \tag{4}$$

Nodal reparametrisation

A reduction of the system to its minimal possible dimension can be achieved by expressing $\boldsymbol{q}_n$ in terms of discrete gerneralised coordinates $\boldsymbol{u}_n \in U \subseteq \mathbb{R}^{n-m}$, such that the constraints are fulfilled via the map $\boldsymbol{F} : U \times Q \to C \subseteq \mathbb{R}^n$.

$$\boldsymbol{q}_n = \boldsymbol{F}(\boldsymbol{u}_n, \boldsymbol{q}_{n-1}) \qquad \text{with} \qquad \boldsymbol{g}(\boldsymbol{q}_n) = \boldsymbol{g}(\boldsymbol{F}(\boldsymbol{u}_n, \boldsymbol{q}_{n-1})) = \boldsymbol{0}$$

Inserting this in the reduced discrete equations of motion (4) further reduces the system to $(n-m)$ equations.

$$\boldsymbol{P}^T(\boldsymbol{q}_n) \cdot \left(D_2 L_d(\boldsymbol{q}_{n-1}, \boldsymbol{q}_n) + D_1 L_d(\boldsymbol{q}_n, \boldsymbol{F}(\boldsymbol{u}_{n+1}, \boldsymbol{q}_n)) + \boldsymbol{f}_{n-1}^+ + \boldsymbol{f}_n^- \right) = \boldsymbol{0} \tag{5}$$

Since the control forces $\boldsymbol{f}$ are applied to the n-dimensional redundant configuration $\boldsymbol{q}$, they can be computed via

$$\boldsymbol{f}_{n-1}^+ = \frac{\Delta t}{2} \boldsymbol{B}^T(\boldsymbol{q}_n) \cdot \boldsymbol{\tau}_{n-1} \qquad \text{and} \qquad \boldsymbol{f}_n^- = \frac{\Delta t}{2} \boldsymbol{B}^T(\boldsymbol{q}_n) \cdot \boldsymbol{\tau}_n$$

with the $n \times (n-m)$ configuration dependent input transformation matrix $\boldsymbol{B}$ and the discrete generalised forces $\boldsymbol{\tau}_n$ (being assumed to be constant during a time interval). At each time node, the control forces can be computed as $\boldsymbol{f}_n = \boldsymbol{f}_n^+ + \boldsymbol{f}_n^-$.

3 OPTIMAL CONTROL PROBLEM

With the derived equations of motion both for continuous (2) and discrete (5) forced constrained systems, we can now formulate the optimal control problem.

3.1 Optimal control of constrained motion

The goal is to find an optimal trajectory of state and control, minimising the objective function

$$J(\boldsymbol{q}, \dot{\boldsymbol{q}}, \boldsymbol{f}) = \int_{t_0}^{t_N} C(\boldsymbol{q}, \dot{\boldsymbol{q}}, \boldsymbol{f})\, dt$$

with a given continuous cost function $C(\boldsymbol{q}, \dot{\boldsymbol{q}}, \boldsymbol{f}) : T_{\boldsymbol{q}}Q \times \mathbb{R}^n \to \mathbb{R}$, subject to constraints, consisting of the fulfilment of equations of motion (2), initial and final values for both configuration $\boldsymbol{q}_0 = \boldsymbol{q}(t_0)$, $\boldsymbol{q}_N = \boldsymbol{q}(t_N)$, and velocity $\dot{\boldsymbol{q}}_0 = \dot{\boldsymbol{q}}(t_0)$, $\dot{\boldsymbol{q}}_N = \dot{\boldsymbol{q}}(t_N)$ and path constraints $\boldsymbol{0} \leq \boldsymbol{h}(\boldsymbol{q}, \dot{\boldsymbol{q}}, \boldsymbol{f})$.

3.2 Discrete mechanics and optimal control of constrained systems DMOCC

As described in [8], we can now formulate the optimal control problem for discrete constrained motion related to the reduced discrete equations of motion (5). First, we introduce the approximation

$$C_d(\boldsymbol{q}_n, \boldsymbol{q}_{n+1}, \boldsymbol{f}_n) \approx \int_{t_n}^{t_{n+1}} C(\boldsymbol{q}, \dot{\boldsymbol{q}}, \boldsymbol{f})\, dt$$

Examples of the approximation of the integrated continuous objective function by C_d are described in Section 3.3. As in the continuous case, the goal is to find an optimal discrete trajectories $\boldsymbol{q}_d = \{\boldsymbol{q}_n\}_{n=0}^N$ and $\boldsymbol{f}_d = \{\boldsymbol{f}_n\}_{n=0}^{N-1}$, that minimise the discrete objective function

$$J_d(\boldsymbol{q}_d, \boldsymbol{f}_d) = \sum_{n=0}^{N-1} C_d(\boldsymbol{q}_n, \boldsymbol{q}_{n+1}, \boldsymbol{f}_n)$$

or alternatively in generalised quantities $\boldsymbol{u}_d = \{\boldsymbol{u}_n\}_{n=0}^N$ and $\boldsymbol{\tau}_d = \{\boldsymbol{\tau}_n\}_{n=0}^{N-1}$,

$$\overline{J}_d(\boldsymbol{u}_d, \boldsymbol{\tau}_d) = \sum_{n=0}^{N-1} \overline{C}_d(\boldsymbol{u}_n, \boldsymbol{u}_{n+1}, \boldsymbol{\tau}_n)$$

while at the same time fulfilling the reduced discrete equations of motion (5), discrete path constraints $\mathbf{0} \leq \boldsymbol{h}_d(\boldsymbol{q}_n, \boldsymbol{q}_{n+1}, \boldsymbol{f}_n)$ and the initial and final values for both configuration and velocity given above. Note that the initial and final velocity conditions are transformed into conditions on the conjugate momentum $\boldsymbol{p}_0 = \boldsymbol{p}(t_0)$, $\boldsymbol{p}_N = \boldsymbol{p}(t_N)$, respectively. The dimension of the optimal control problem in the discrete setting is minimal due to the equations of motion being reduced via the discrete null space method and nodal reparametrisation of configuration and force.

3.3 Physiologically motivated cost functions

To get reasonable trajectories of state and control from the optimisation of the index finger movement, we investigate physiologically motivated cost functions. In this work we compare four different cost functions and their effect on the index finger trajectory. The actuation of the finger due to muscles is currently simply represented by bounded joint torques. However, the inclusion of muscle models and tendons is planned for the future.

Minimum control effort Minimising the control effort is an often used criterion in control and feedback control applications. In a physiological sense, it can be understood as a minimum muscle force effort ncecessary to control the motion. In discrete generalised coordinates, the optimal control problem for this criterion can be formulated as

$$\overline{J}_d = \Delta t \sum_{n=1}^{N-1} \boldsymbol{\tau}_n^T \cdot \boldsymbol{\tau}_n$$

Minimum torque change Minimum torque change during a body movement means that the activation level of muscles is exposed to minimal changes. In particular, a minimal number of motor units of the muscles changes their activation level. For more details on that topic, see [9]. Thus, this criterion can be interpreted as a minimum activation effort of muscle motor units. The appropriate objective function is given by

$$\overline{J}_d = \frac{1}{2}\Delta t \sum_{n=1}^{N-2} (\frac{\boldsymbol{\tau}_{n+1} - \boldsymbol{\tau}_n}{\Delta t})^T \cdot (\frac{\boldsymbol{\tau}_{n+1} - \boldsymbol{\tau}_n}{\Delta t})$$

Minimum kinetic energy In order to minimise integral over the kinetic energy, velocities during the movement have to be minimised, in particular that of the heaviest body. In our case, as we use constant time steps, this results in minimal distances per timestep. Denoting the system's mass matrix by $\boldsymbol{M}$, the following objective function is used for this criterion

$$\overline{J}_d = \frac{1}{2}\Delta t \sum_{n=0}^{N} \boldsymbol{p}_n^T \cdot \boldsymbol{M}^{-1} \cdot \boldsymbol{p}_n$$

Minimum jerk in fingertip The jerk is the derivative of acceleration with respect to time. Hence, this criterion leads to a motion with minimal changes in the acceleration of the fingertip. To achieve this, we calculate the discrete actual arc length s_n from the change in location of the fingertip $\boldsymbol{x}_f$ during one time step $s_n = \boldsymbol{x}_{f_{n+1}} - \boldsymbol{x}_{f_n}$ and apply finite differences to gain the third derivative with respect to time s_n'''. The related objective function is

$$\overline{J}_d = \Delta t \sum_{n=1}^{N-2} (s_n''')^2$$

4 MODEL

The proximal interphalangeal joint and the distal interphalangeal joint combining the medial and distal phalanxes to the finger allow rotation around one axis to perform flexion-extension, only. The proximal and

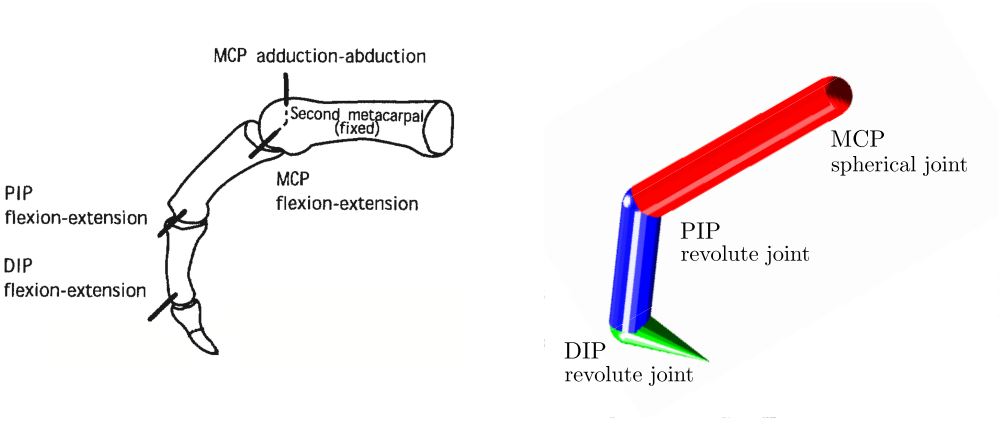

Figure 2. Illustration of the index finger from [14] (left) and the model of the index finger used in this study (right).

equality constraints	
equations of motion	$\boldsymbol{P}^T(\boldsymbol{q}_n) \cdot \left(D_2 L_d(\boldsymbol{q}_{n-1}, \boldsymbol{q}_n) + D_1 L_d(\boldsymbol{q}_n, \boldsymbol{F}(\boldsymbol{u}_{n+1}, \boldsymbol{q}_n)) + \boldsymbol{f}_{n-1}^+ + \boldsymbol{f}_n^-\right) = \boldsymbol{0}$
initial configuration	$\boldsymbol{u}_0 = \boldsymbol{0}$
initial momentum	$\boldsymbol{p}_0 = \boldsymbol{0}$
final momentum	$\boldsymbol{p}_N = \boldsymbol{0}$
final location of the fingertip	$\boldsymbol{x}_{f_N} = [0, 0.049, 0.04]$

inequality constraints	
joint angle MCP	$-45° \leq \alpha \leq 45°$
joint angle PIP	$0° \leq \beta \leq 100°$
joint angle DIP	$0° \leq \gamma \leq 70°$

Table 1. Equality and inequality constraints on the optimal control problem of index finger movements.

medial phalanxes are modelled as cylinders, the distal phalanx is modelled as a cone, all of them with radii and lengths taken approximately from [3].
The rotational degrees of freedom of each rigid body are described in terms of a rotation matrix whose columns are orthonormal directors giving rise to so called internal constraints. The restriction of the relative motion of neighbouring bodies due to interconnecting joints yields external constraints.
The optimal control problem is formulated as the minimisation of different cost functions subject to constraints as described in Section 3. We want to simulate a rest to rest grasping manoeuvre, hence initial momentum $\boldsymbol{p}_0$ and final momentum $\boldsymbol{p}_N$ are zero. The movement ought to start at a specified outstretched horizontal position $\boldsymbol{u}_0 = \boldsymbol{0}$ (characterised relative to a reference configuration) and the fingertip must arrive at a final position $\boldsymbol{x}_{f_N}$ at the end of the movement. Furthermore, bounds on possible angles between the phalanxes yield inequality constraints. A summary of the constraints is given in Table 1.

5 RESULTS

Solving the optimal control problem with different cost functions leads to different trajectories of the fingertip, see left hand plot in Figure 3. In case of minimum control effort, the fingertip follows a rather unrealistic trajectory. The fingertip stays for a long time on the initial level of potential energy and approaches the final position only during the last steps. The trajectories resulting from the minimum torque change and minimum kinetic energy criterion look quite similar to each other, only during the last time steps, the minimum kinetic energy trajectory is more flat. The minimum jerk criterion leads to a trajectory that is much less

curved. In [6] it is stated that fingers tend to follow a logarithmic spiral during grasping. If we compare the absolute differences of the resulting trajectories to a logarithmic spiral through start end end point of the movement, see right hand plot in Figure 3, we can say that the minimum angular jerk and minimum kinetic energy criterions are best fitting. This is also observable from the averaged absolute differences between the curves and the logarithmic spiral, see Table 2. Looking at the slope of the curves, one can see that all three criterions minimum torque change, minimum kinetic energy and minimum jerk in fingertip lead to trajectories that have only small absolute differences with respect to the slope of the logarithmic spiral. Especially during the middle part of the motion, the slope of the minimum torque change curve is nearly equal to that of logarithmic spiral. But as the differences in beginning and end of the movement are very high for this criterion, Table 2 shows that the minimum kinetic energy criterion is on average best fitting to the slope of the logarithmic spiral.

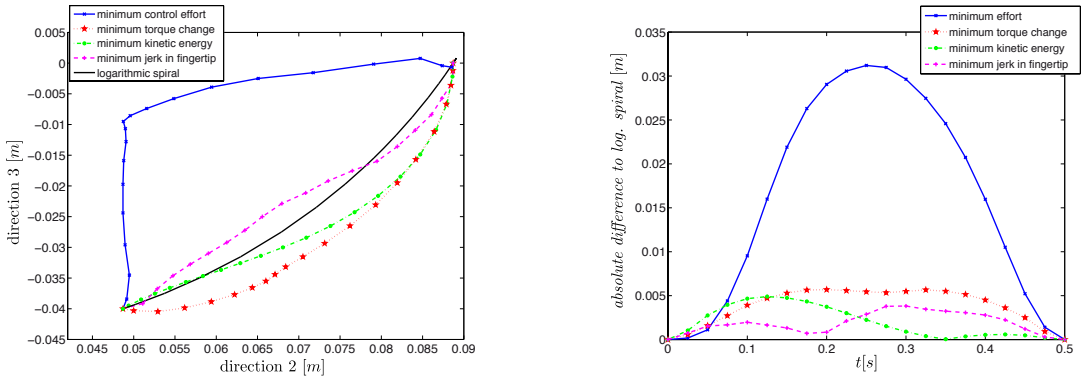

Figure 3. Optimal index finger trajectories for different cost functions (left) and absolute difference of optimal trajectories with respect to a logarithmic spiral (right).

cost function	**absolute difference [m]**	**difference in slope [m/s]**
minimum effort	0.0160	0.1317
minimum torque change	0.0038	0.0269
minimum kinetic energy	0.0019	0.0226
minimum jerk in fingertip	0.0019	0.0251

Table 2. Comparison to logarithmic spiral: averaged absolute differences of fingertip trajectory and slope for different cost functions.

From Figure 4 one can see, that in case of a minimum control effort criterion, the finger is actuated in particular during the first time steps in the first joint, to accelerate upwards. Then, during long times of the motion, the torques in the first joint are reduced to a minimal level and finally, the finger uses gravity to get to the final point and is decelerated by ascending torques in the first joint during the last time steps. The cost function minimum torque change naturally leads to hardly changing torques over time in all joints, the MCP torques are actually nearly constant. For the minimum kinetic energy criterion, the evolution of torques is similar to that resulting from the minimum torque change criterion, but allowing a bit higher changes in the torques. A movement with minimum jerk in the fingertip leads to comparatively high values and changes in all joint torques in order to keep the fingertip at a constant acceleration.
In Figure 5, kinetic energy and jerk in the fingertip are shown resulting from the different cost functions. One can clearly recognise, that the other cost functions result in substantially higher values of kinetic energy (left hand plot) and jerk (right hand plot). The configurations of the whole finger during grasping are depicted in Table 3 at four particular times during the movement to show the effect of the different cost functions on the total index finger movement.

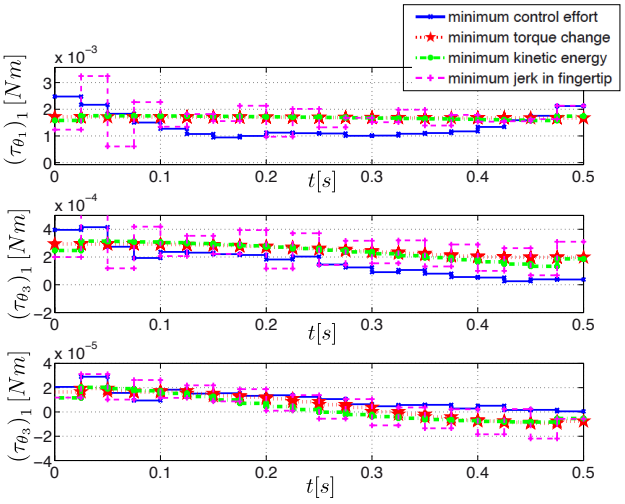

Figure 4. Evolution of torques in joints in direction of grasping movement for different cost functions.

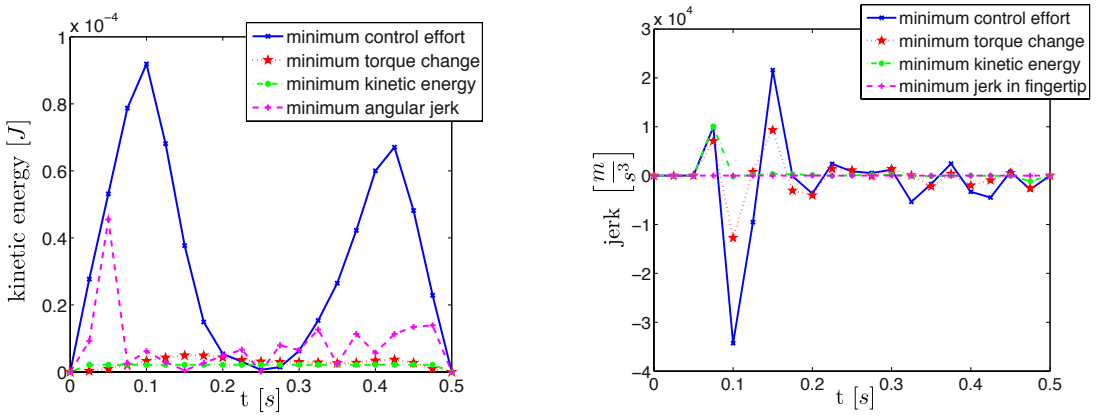

Figure 5. Kinetic energy (left) and jerk in fingertip (right) of movements resulting from different cost functions.

6 CONCLUSIONS

In this work, we simulate grasping movements of the index finger with discrete mechanics and optimal control for constrained systems and used different physiologically motivated cost functions in the optimal control problem. Concluding, we can say, that the minimum control effort criterion does not lead to reasonable grasping movements at this stage. Perhaps this changes, when muscles and tendons are included in the model and attention is paid to the fact that not all joints can move independently from each other. Comparing our results to the statement from [6], we see that trajectories resulting from the minimum kinetic energy and minimum angular jerk criterion are both fitting equally well to a logarithmic spiral from start to the endpoint of the movement. The minimum kinetic energy cost function actually leads to a slightly better fitting of the slope of the curve. The slope of the trajectory resulting from the minimum torque change criterion is also very similar to that of the logarithmic spiral, in particular during the middle part of the movement. In future work we plan to include muscle models as described for example in [11]. Furthermore, we want to use more realistic geometries to represent the bones and moments of inertia. Moreover, other finger or hand movements like low impact piano playing are interesting movements to be examined.

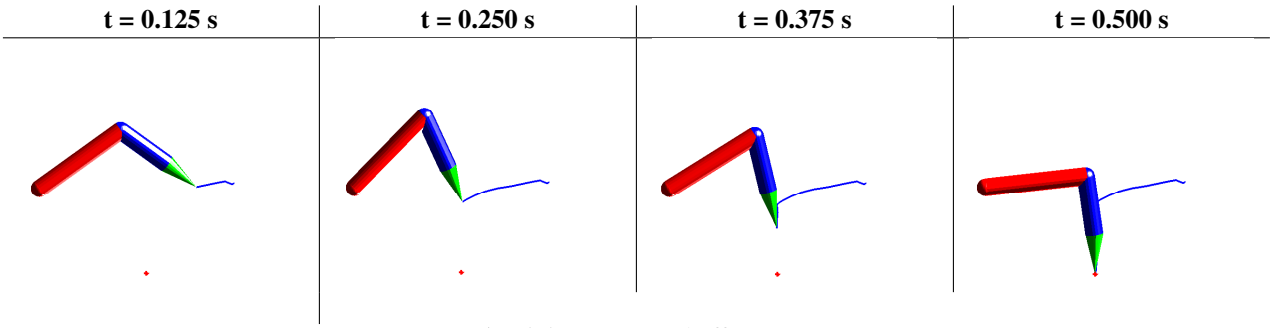

a) Minimum control effort.

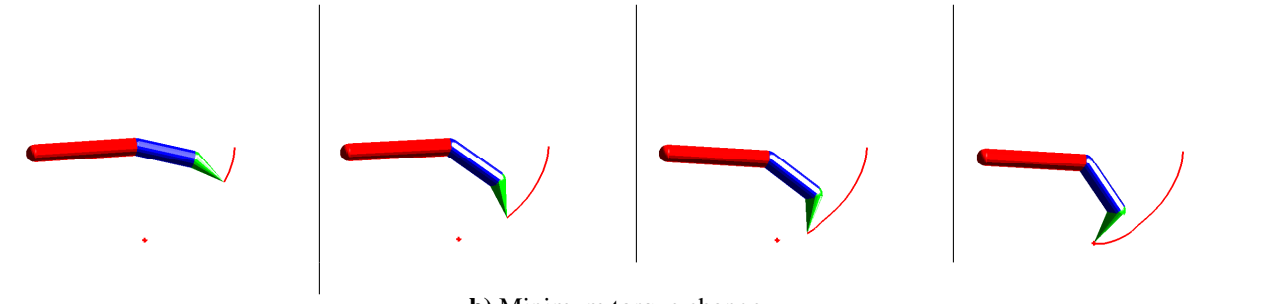

b) Minimum torque change.

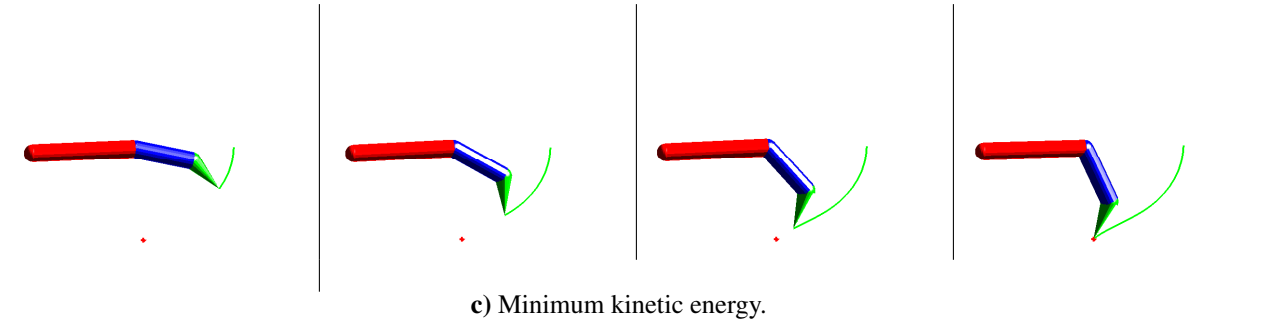

c) Minimum kinetic energy.

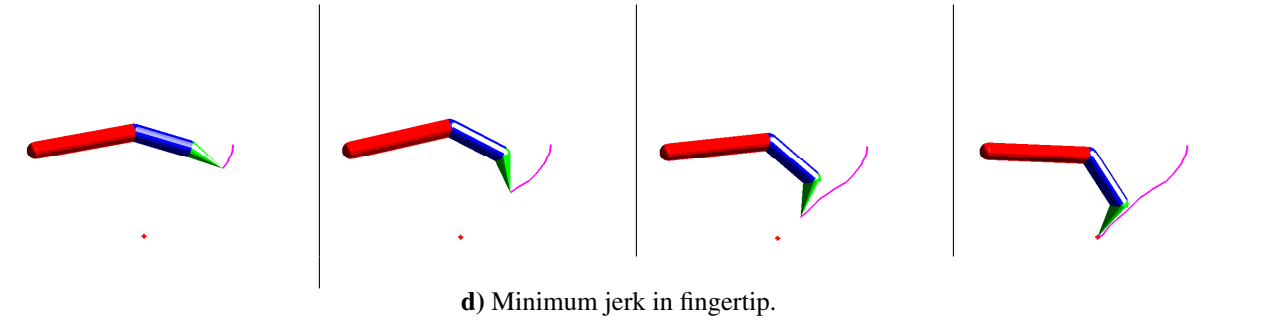

d) Minimum jerk in fingertip.

Table 3. Finger movements during grasping for different cost functions: a) minimum control effort, b) minimum torque change, c) minimum kinetic energy and d) minimum jerk in fingertip. From left to right, the finger configuration is shown at four typical time steps.

REFERENCES

[1] BETSCH, P., AND LEYENDECKER, S. The discrete null space method for the energy consistent integration of constrained mechanical systems. Part II: Multibody dynamics. *International Journal for Numerical Methods in Engineering 67*, 4 (2006), 499–552.

[2] BIESS, A., LIEBERMANN, D., AND FLASH, T. A computational model for redundant human three-dimensional pointing movements: Integration of independent spatial and temporal motor plans simplifies movement dynamics. *The Journal of Neuroscience 27*, 48 (2007), 13045–13064.

[3] BUCHHOLZ, B., ARMSTRONG, T. J., AND GOLDSTEIN, S. A. Anthrophometric data for describing the kinematics of the human hand. *Ergonomics 35*, 3 (1992), 261–273.

[4] FRIEDMAN, J., AND FLASH, T. Trajectory of the index finger during grasping. *Experimental Brain Research 196*, 4 (2009), 497–509.

[5] GRAY, H. *Anatomy of the human body*, 20 ed. Philadelphia: Lea & Febiger, 1918.

[6] KAMPER, D., CRUZ, E., AND SIEGEL, M. Stereotypical fingertip trajectories during grasp. *The Journal of Neurophysiology 90*, 6 (2003), 3702–3710.

[7] LEYENDECKER, S., MARSDEN, J. E., AND ORTIZ, M. Variational integrators for constrained dynamical systems. *Zeitschrift für Angewandte Mathematik und Mechanik 88*, 9 (2008), 677–708.

[8] LEYENDECKER, S., OBER-BLÖBAUM, S., MARSDEN, J. E., AND ORTIZ, M. Discrete mechanics and optimal control for constrained systems. *Optimal Control Applications & Methods* (2009). DOI: 10.1002/oca.912.

[9] LINKE, W., AND PFITZER, G. Kontraktionsmechanismen. In *Physiologie des Menschen*, 30 ed. Springer, Berlin Heidelberg, 2007, pp. 111–139.

[10] MARSDEN, J. E., AND WEST, M. Discrete mechanics and variational integrators. *Acta Numerica 10* (2001), 357–514.

[11] SIEBERT, T., RODE, C., HERZOG, W., TILL, O., AND BLICKHAN, R. Nonlinearities make a difference: comparison of two commonhill-type models with real muscle. *Biological Cybernetics 98*, 2 (2008), 133–143.

[12] SOECHTING, J., BUNEO, C., HERRMANN, U., AND FLANDERS, M. Moving effortlessly in three dimensions: does Donder's law apply to arm movement? *The Journal of Neuroscience 15*, 9 (1995), 6271–6280.

[13] SPITZER, M. Geist in Bewegung. *Nervenheilkunde 28*, 6 (1985), 403–405.

[14] VALERO-CUEVAS, F. J. Applying principles of robotics to understand the biomechanics, neuromuscular control and clinical rehabilitation of human digits. In *Proceedings of the 2000 IEEE International Conference on Robotics & Automation* (San Francisco, California, 24-28 April 2000), I. R. . A. Society, Ed., IEEE, 2000.